MIMICAD TECHNICAL REPORT NO. 3

Calculation of Transmission Line Parameters and Electric Field Distribution of Coplanar Electrodes on Layered Dielectric Substrates

by

Peter S. Weitzman, J.M. Dunn and
A.R. Mickelson

Department of Electrical and Computer Engineering
University of Colorado
Boulder, Colorado 80309-0425

Work described in this report has been supported by the Martin Marietta Corporation, the Office of Naval Research, the Army Research Office, and the National Science Foundation

May 1990

Acknowledgements

The authors would like to acknowledge the Martin Marietta Corporation for providing the microwave optics fellowship which supported some of the research done for this report. We also acknowledge the support of the Office of Naval Research (N0014-88-K-0685), The Army Research Office (DAAL03-88-K-0053), and the National Science Foundation grant to the MIMICAD Center (CDR-8722832).

Abstract

A numerical technique for calculating the electric field distribution and capacitance of coplanar strip electrodes placed on top of a layered dielectric substrate is presented. A Green's function for the potential due to a point charge in the plane of the electrodes is found using Fourier transform techniques. The charge distribution on the electrodes is calculated by solving an integral equation. The static capacitance is calculated by integrating the charge distribution. The electric field at any point in the substrate can be found by integrating the charge distribution times the Green's function.

1 Introduction

The analysis of coplanar transmission lines and electrode structures has been studied extensively in recent years. Coplanar electrodes are used in any MMIC structure involving FETs, and in integrated optic devices. In many devices, coplanar electrodes are placed on a layered dielectric substrate. The modeling of coplanar electrode structures requires knowledge of the transmission line properties of the devices and in some cases the electric field distribution in the substrate. In order to analyze the performance of electro-optic

devices, the transmission line properties of the electrodes must be calculated. It is also useful to calculate the fields generated in the electro-optic material in order to determine how much power is needed to achieve the desired electro-optic effect. When the electrodes are placed directly on top of the electro-optic substrate, the line capacitance and fields can be found in closed form by conformal mapping. This is the case when ITO(Indium Tin Oxide) electrodes are used since they act as a buffer layer for optical frequencies and conductors at microwave frequencies. Gupta [1] calculates the static capacitance of coplanar strip electrodes. Ramer [2] uses conformal mapping to calculate the static electric fields generated by coplanar strip electrodes in the absence of a buffer layer.

When metal electrodes are used, a dielectric buffer layer must be placed between the electrodes and the substrate to avoid attenuation of the light by the metal. Conformal mapping is not applicable to solving this problem when a buffer layer is present. Several approaches to this problem have been presented recently. Knorr and Kuchler [3] use a spectral domain technique to find the transmission line parameters of coplanar strip electrodes on a layered dielectric substrate. Thylen and Granestrand [4] use an iterative approach

to calculate the electric field in the substrate. Kuester [5] uses an integral equation approach to find an approximation for the static capacitance of the electrodes. Marcuse [6] uses a point matching technique to solve for the electric field in the substrate. Sabatier and Caquot [7] use the method of images to find approximations for the electric field in the substrate as well as the buffer layer.

In this paper, we present a numerical technique for computing the electric field and line capacitance of coplanar strip electrodes with a dielectric buffer layer present. All calculations are based on the quasi static approximation since optical modulators have dimensions much smaller than the microwave wavelengths currently being used in these applications. First the Green's functions for the potential in the plane of the electrodes and the field components in the substrate due to a charge in the plane of the electrodes are found. The Green's function is then used to solve an integral equation for the charge on the electrodes using the method of moments. Once the charge is known, the capacitance can be found by integrating the charge. The field components in the substrate can be found by integrating the charge times the Green's function for the fields. This paper will present a comparison between

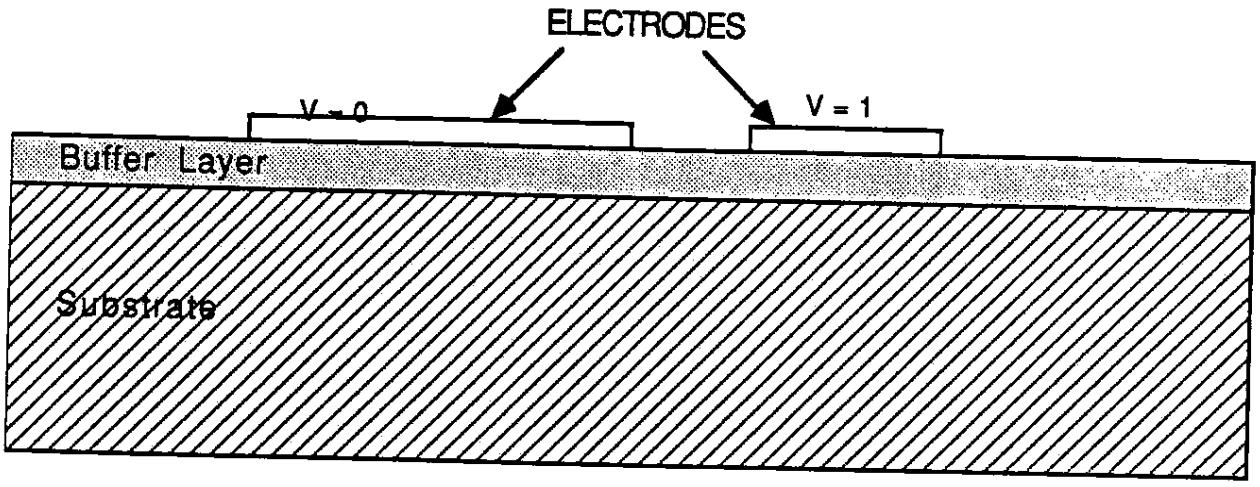

Figure 1: The structure to be analyzed

these numerical results, other published results and some experimental data.

2 Green's functions in the three layer dielectric

The structure to be analyzed is shown in Figure 1. The electrodes are assumed to be infinitely thin, and the substrate is assumed to be infinitely thick.

The Green's function for this problem corresponds to the potential due to a point charge in the plane of the electrodes. The problem is divided into four regions (see Figure 2). Region one is free space ($\epsilon_r = 1$) above the point

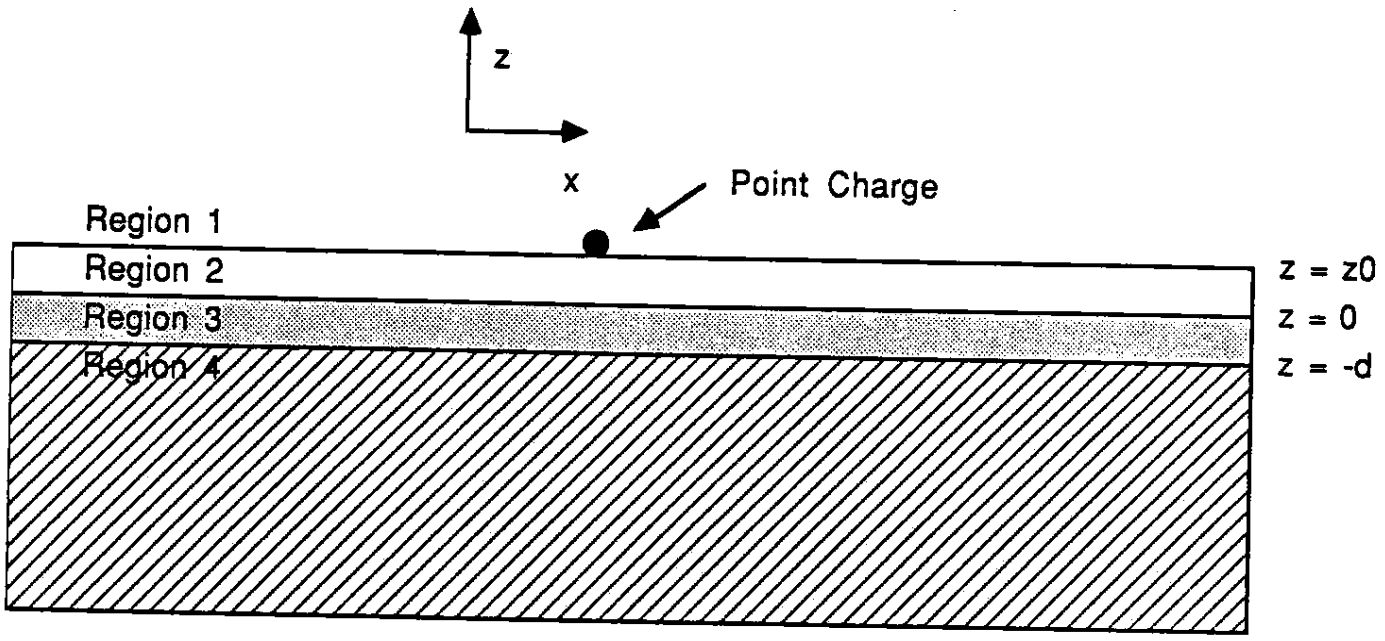

Figure 2: The four regions and coordinate system used to find the Green's function

charge. Region two is also free space, below the point charge but above the buffer layer. Region two must be included to have sufficient boundary conditions, then the limit where the thickness of region two approaches zero is taken. Region three is the buffer layer ($\epsilon_r = \epsilon_b$) and region four is the substrate ($\epsilon_r = \epsilon_s$). Finding the Green's function therefore amounts to solving the Poisson equation The Green's function is the solution of the Poisson

$$\frac{\partial^2 G}{\partial x^2} + \frac{\partial^2 G}{\partial z^2} = \frac{\delta(x - x_0)\delta(z - z_0)}{\epsilon_0} \tag{1}$$

With the boundary conditions

$$G(x, x_0, z, z_0) = 0 \text{ at } z = \pm\infty \tag{2}$$

$$G(x, x_0, z, z_0) \text{ is continuous across dielectric boundaries} \tag{3}$$

$$G(x, x_0, z, z_0) \text{ is continuous across the point charge} \tag{4}$$

$$\epsilon \frac{\partial G}{\partial z} \text{ is continuous across boundaries} \tag{5}$$

and

$$\int_{z_0-}^{z_0+} G(x, x_0, z, z_0) = \frac{\delta(x - x_0)}{\epsilon_0} \tag{6}$$

Taking the Fourier transform in x of equation 1. yields the equation

$$\frac{\partial^2 \overline{G}}{\partial z^2} - \xi^2 \overline{G} = \frac{e^{-j\xi x_0}\delta(z - z_0)}{\epsilon_0} \tag{7}$$

The first four boundary conditions transform to identical forms, however the fifth one (6) transforms to the form

$$\int_{z_0-}^{z_0+} G(\xi, x_0, z, z_0) = \frac{e^{-j\xi x_0}}{\epsilon_0} \tag{8}$$

The homogeneous solution to this equation is

$$\overline{G}(\xi, x_0, z, z_0) = Ae^{-|\xi|(z-z_0)} + Be^{|\xi|(z-z_0)} \tag{9}$$

Applying this homogeneous solution in each of the four regions results in eight equations and eight unknowns. Fortunately the boundary conditions (2 - 6) provide eight equations. Solving this system of equations, then setting $z_0 = 0$ to put the charge in the plane of the electrodes, and taking the inverse Fourier transform gives the following solution for the Greens function.

In the substrate:

$$G(\xi, x_0, z, 0) = \frac{1}{4\pi\epsilon_0} \int_{-\infty}^{+\infty} \frac{e^{j\xi(x-x_0)} e^{-|\xi|z} F(\xi) d\xi}{|\xi|} \tag{10}$$

where

$$F(\xi) = \frac{1}{(\epsilon_b - 1)(1 - \frac{\epsilon_s}{\epsilon_b})e^{-2|\xi|d} - 1 - \frac{\epsilon_s}{\epsilon_b} - \epsilon_b - \epsilon_s} \tag{11}$$

which can be written

$$F(\xi) = \frac{1}{Ce^{-2|\xi|d} - D} \tag{12}$$

where

$$C = (\epsilon_b - 1)(1 - \frac{\epsilon_s}{\epsilon_b}) \tag{13}$$

$$D = 1 + \frac{\epsilon_s}{\epsilon_b} + \epsilon_b + \epsilon_s \tag{14}$$

taking out a factor $1/D$ results in

$$F(\xi) = \frac{1}{D}\frac{1}{1-\frac{C}{D}e^{-2|\xi|d}} \tag{15}$$

using the equality

$$\frac{1}{1-x} = 1 + x + x^2 + x^3 + \ldots \tag{16}$$

$F(\xi)$ can be reduced to

$$F(\xi) = \sum_{n=0}^{\infty} \frac{1}{D}(\frac{C}{D})^n e^{-2n|\xi|d} \tag{17}$$

using the fact that

$$e^{J\xi(x-x0)} = \cos\xi(x-x_0) + j\sin\xi(x-x_0) \tag{18}$$

and the sine terms drop out because sine is an even function and the integration is from $-\infty$ to $+\infty$ the integral becomes

$$G(\xi, x_0, z, 0) = \frac{1}{2\pi\epsilon_0}\sum_{n=0}^{\infty}\int_0^{+\infty}\frac{1}{D}(\frac{C}{D})^n\frac{cos\xi(x-x_0)e^{-|\xi|(z+2nd)}d\xi}{|\,\xi\,|} \tag{19}$$

now to solve the integral in equation 19 we let

$$I = \int_0^{\infty}\frac{\cos axe^{-bx}dx}{x} \tag{20}$$

$$\frac{dI}{dB} = -\int_0^{\infty}\cos axe^{-bx}dx \tag{21}$$

using the identity

$$\int_0^\infty e^{-px}\cos(qx+\lambda)dx = \frac{1}{p^2+q^2}(p\cos(\lambda)-q\sin(\lambda))[8] \qquad (22)$$

yields

$$\frac{dI}{db} = -\frac{b}{b^2+A^2} \qquad (23)$$

integrating with respect to b gives the result

$$I = -\frac{1}{2}\ln \mid a^2+b^2 \mid \qquad (24)$$

using the results from equations (24) and (19) yields the following result for the Green's function

$$G(x,x0,z,0) = \frac{1}{D}\sum_{n=0}^{\infty}(C/D)^n \ln \mid (x-x_0)^2+(z+2nd)^2 \mid \qquad (25)$$

Similarly the Green's function in the plane of the electrodes is found to be

$$\begin{aligned} G(x,x_0) &= \frac{1}{2\pi\epsilon_0}[\ln(x-x_0) - 1/2\sum_{n=0}^{\infty}(C/D)^n[(A/D)\ln((x-x_0)^2 + \\ &\quad (2(n+1)d)^2) + (B/D)\ln((x-x_0)^2+(2nd)^2)]] \end{aligned}$$

where C and D are the same as above and

$$A = \epsilon_s - \epsilon_b \qquad (26)$$

and

$$B = \epsilon_s + \epsilon_b \tag{27}$$

For a typical case of $LiNbO_3$ substrate and SiO_2 buffer layer $\epsilon_s = 34.7$, $\epsilon_b = 3.9$, $\frac{C}{D} = 0.47$ $(\frac{C}{D})^n \approx 10^{-5}$ for n = 15. I used 15 terms to approximate the infinite series.

Since $\overline{E} = - \bigtriangledown \Phi$, the Green's functions for the x and z directed fields can be found by taking the x and z derivatives of the Green's function for the potential. The x component of electric field in the substrate generated by a point charge in the plane of the electrodes is given by:

$$E_x(x, x_0, z) = -(1/D) \sum_{n=0}^{\infty} (C/D)^n \frac{2(x - x_0)}{(x - x_0)^2 + (z - z_0 + (2nd))^2} \qquad (28)$$

Similarly the Green's function for the z component is given by

$$E_z(x, x0, z) = -(1/D) \sum_{n=0}^{\infty} (C/D)^n \frac{2(z - z_0 + 2nd)}{(x - x_0)^2 + (z - z_0 + (2nd))^2} \qquad (29)$$

where C and D are given by equations (13) and (14). For an SiO_2 buffer layer ($\epsilon = 3.9$) with a $LiNbO_3$ substrate ($\epsilon = 34.7$), $\frac{C}{D} = -0.47$ which means that only about fifteen terms of the infinite series are needed to get five place accuracy.

3 Computation of charge distribution on coplanar electrodes

The first step in the numerical process is to compute the charge density on the electrodes. Computing the charge distribution is unique to this method

of solution. This is done by solving the integral equation

$$V(x) = \int_{\text{left electrode}} \sigma(x')G(x,x')dx' + \int_{\text{right electrode}} \sigma(x')G(x,x')dx' \tag{30}$$

where $\sigma(x)$ is the charge distribution, G is the Green's function (26) found in the last section and $V(x)$ is zero on the left electrode and unity on the right electrode. Due to the linearity of the problem, if the voltage on the right electrode is multiplied by a constant, the fields will be multiplied by the same constant.

Equation (30) is then solved by the method of moments. We chose to use Dirac delta functions as both basis and weighting functions so that all integration could be performed in closed form. The solution is obtained in the following way.

$$\sigma(x) = \sum_{i=1}^{n} \sigma_i b_i(x) \tag{31}$$

$$b_i(x) = \delta(x - x_i) \text{ where the } x_i\text{s are equally spaced along the electrodes} \tag{32}$$

$$w_j(x) = \delta(x - x_j) \text{ where the } x_j\text{s are equally spaced along the electrodes but offset from the } x_i\text{s} \tag{33}$$

The integral equation is then reduced to the matrix equation

$$[L][u] = [v] \tag{34}$$

where L is the known n by n matrix with elements

$$\begin{aligned} L_{i,j} &= \int_{electrodes} Lb_i(x) w_j(x) dx & (35) \\ &= Lb_i(x) \mid_{x=x_j} & (36) \\ &= \int_{electrodes} G(x_j, x') b_i(x') dx' & (37) \\ &= G(x_j, x_i) & (38) \end{aligned}$$

u is the unknown vector which contains the solution for the charge density (the σ_is) and v is the known vector which contains the voltages on the electrodes. So solving

$$[u] = [L]^{-1}[v] \tag{39}$$

yields the charge distribution on the electrodes.

In figure 3 the charge distribution on a symmetric electrode structure is plotted. The structure has a three micron gap, symmetric ten micron electrodes and a 0.3 micron buffer layer. The buffer layer is SiO_2 ($\epsilon = 3.9$) and the substrate is $LiNbO_3$ ($\epsilon = 34.7$) Although $LiNbO_3$ is anisotropic it

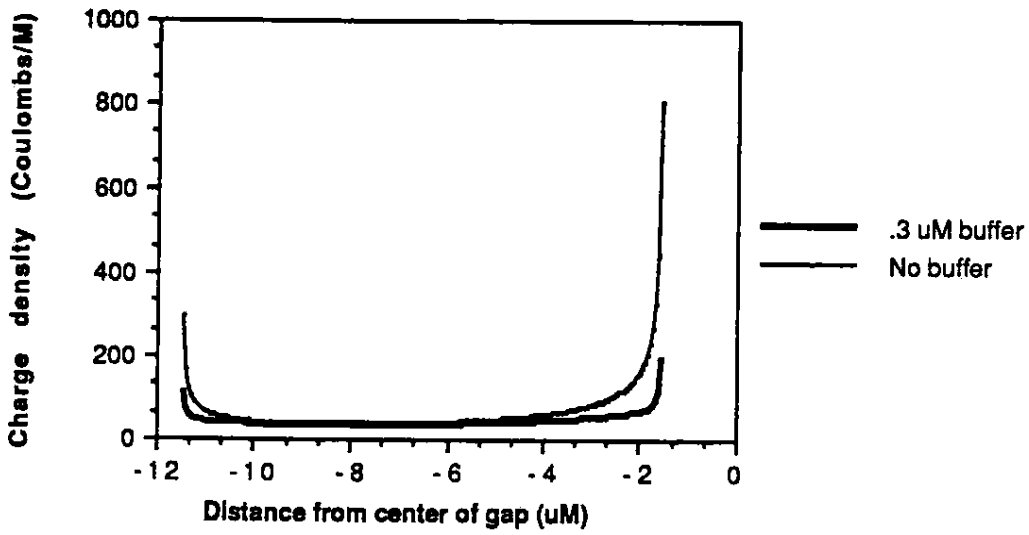

Figure 3: Charge distribution on symmetric coplanar electrodes with three micron gap, and ten micron electrodes

has been shown [9] that letting $\epsilon_s = \sqrt{\epsilon_x \epsilon_y}$ does not change the capacitance or charge distribution.

From figure 3 it is clear that adding a buffer layer tends to flatten out the charge distribution, reducing the peaks in charge near the edge of the electrode, but has little effect on the flat charge distribution near the center of the electrode.

4 Computation of static capacitance of electrodes

Once the charge distribution on the electrodes is known, the capacitance per unit length is very simple to compute using [5]

$$C = \frac{1}{V} \int_{electrodes} \sigma(x) dx \tag{40}$$

since we have defined the charge using delta functions (31) and defined the voltage across the gap to be unity, the capacitance per unit length is simply

$$C = \sum_{i=0}^{n} \sigma_i \tag{41}$$

Kuester [5] uses an integral equation and perturbation technique to approximate the static capacitance of symmetric coplanar strip electrodes. Kuester's expression for the capacitance is given by

$$C = \frac{C_0(\epsilon_s + 1)/2)}{1 - \frac{C_0}{\epsilon_0} \frac{d}{w} \frac{\epsilon_b^2 - \epsilon_s^2}{\epsilon_b(\epsilon_s + 1)}} \tag{42}$$

Where C_0 is the capacitance of the structure in free space and is given by

$$C_0 = \epsilon_0 \frac{K(k')}{K(k)} \tag{43}$$

where K is the complete elliptic integral of the first kind, and the k is given by

$$k = g/(g + 2w) \tag{44}$$

Width	Gap	Buffer Layer thickness	Numerical capacitance	Kuester's capacitance	% Difference
$30\mu M$	$3\mu M$	0	8.91×10^{-10}	8.86×10^{-10}	0.5
$30\mu M$	$3\mu M$	$0.3\mu M$	6.24×10^{-10}	7.18×10^{-10}	15
$10\mu M$	$3\mu M$	0	3.41×10^{-10}	3.44×10^{-10}	2.8
$10\mu M$	$3\mu M$	$0.3\mu M$	2.19×10^{-10}	2.21×10^{-10}	0.7
$3\mu M$	$3\mu M$	0	2.27×10^{-10}	2.47×10^{-10}	8
$3\mu M$	$3\mu M$	$0.3\mu M$	9.59×10^{-11}	1.06×10^{-10}	9
$1\mu M$	$3\mu M$	0	1.95×10^{-10}	1.80×10^{-10}	7
$1\mu M$	$3\mu M$	$0.3\mu M$	7.31×10^{-11}	4.56×10^{-11}	37

Figure 4: Comparison of numerical method vs Kuester's approximation. Kuester's approximation is exact when the buffer layer thickness is zero and

$$k' = \sqrt{1 - k^2} \tag{45}$$

Figure 4 shows calculations of static capacitance for various electrode structures using both the technique outlined above and Kuester's approximation

The numerical results we obtained for capacitance agree very well with

the exact solution (no buffer layer) for relatively wide electrodes. When the electrodes become close to or smaller than the gap size, the accuracy of our technique is diminished. This is due to the fact that more of the charge becomes concentrated near the edges of the electrodes in these cases. The delta functions are unable to model these rapid changes in charge density. Kuester's approximation [5] also breaks down when the electrodes become narrow due to innacurate modeling of the charge distribution near the edges of the electrodes.

5 Computation of Electric fields in the substrate

The components of the electric field in the substrate can be found using the charge distribution and Green's function calculated above in the following equation

$$E_x(x,z) = \int_{electrodes} \sigma(x')G_x(x,x',z)dx' \tag{46}$$

where $G_x(x,x',z)$ is given in equation (28). and

$$E_z(x,z) = \int_{electrodes} \sigma(x')G_z(x,x',z)dx' \tag{47}$$

where $G_z(x,x')$ is given in equation (29). Figures 5 - 8 show plots of

electric field in the substrate at a depth of one micron comparing our numerical results to the exact solution of Ramer [2] and comparing our numerical results to the approximation of Sabatier and Caquot [7] in the presence of a buffer layer. Figures 9 and 10 show the x and z components of the field with and without a buffer layer. The computation of 46 and 47 can be made considerably faster by noting that when $\mid x - x' \mid >> z$ the Green's functions for a two layer dielectric can be substitued in place of equations 28 and 29. This is given by the much simpler expressions

$$G_x(x, x', z) = \frac{1}{2\pi(\epsilon_s + 1)} \frac{2(x - x')}{(x - x')^2 + (z - z')^2} \tag{48}$$

and

$$G_z(x, x', z) = \frac{1}{2\pi(\epsilon_s + 1)} \frac{2(z - z')}{(x - x')^2 + (z - z')^2} \tag{49}$$

In computation of the integrals in equations 46 and 47 the two layer Green's functions were substituted when $\mid x - x' \mid > 10z$, resulting in less than a one percent error and an improvement of a factor of ten in the speed of calculating the fields.

Figures 5 and 6 show good agreement between our numerical approximation and the exact solution. Figures 7 and 8 show that the approximation by Sabatier and Caquot produces very good results, but are not exact. From

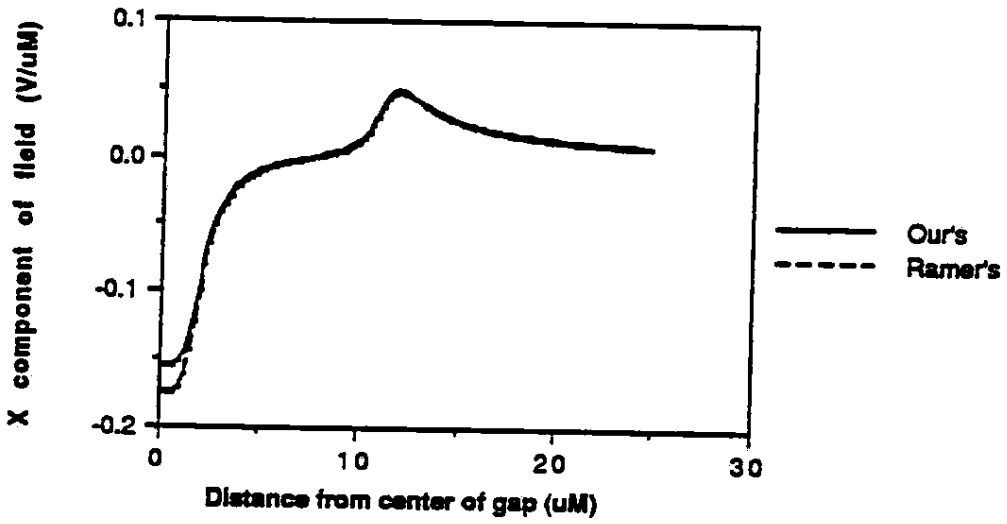

Figure 5: x component of electric field without buffer layer

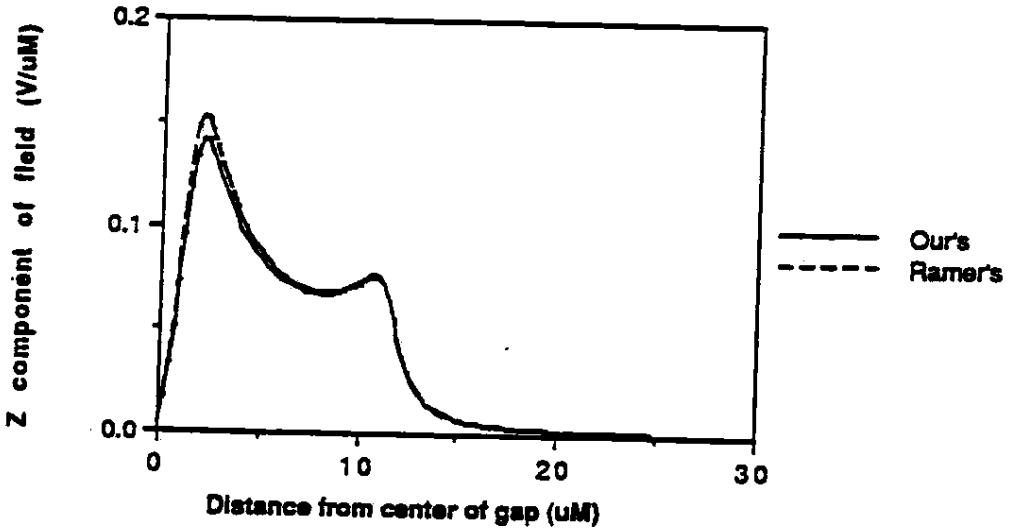

Figure 6: z component of electric field without buffer layer

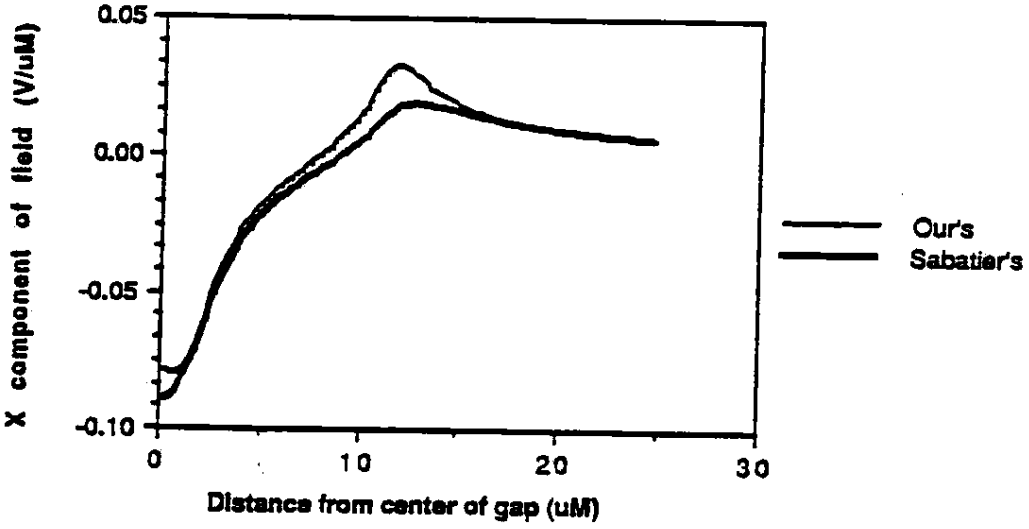

Figure 7: x component of electric field with 0.3 micron buffer layer

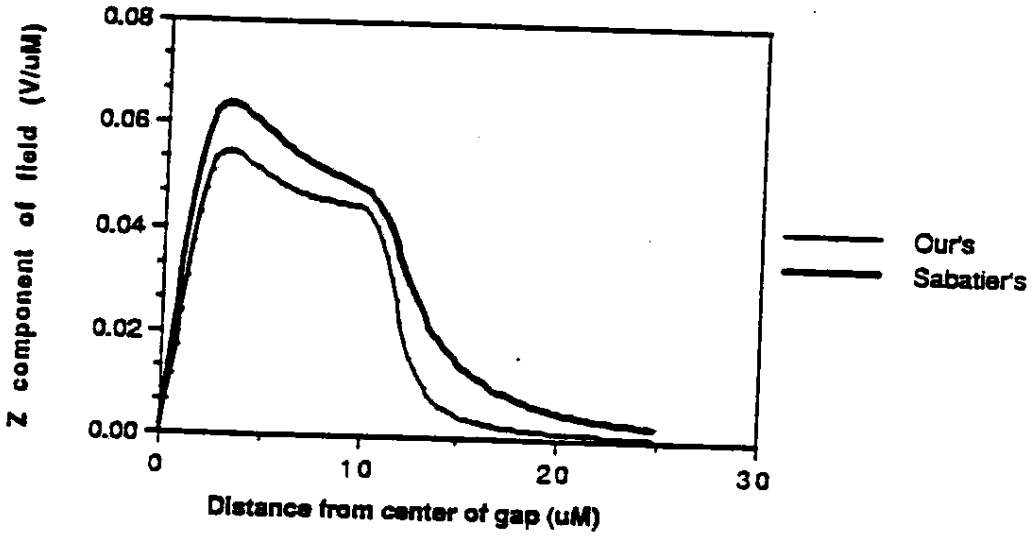

Figure 8: z component of electric field with 0.3 micron buffer layer

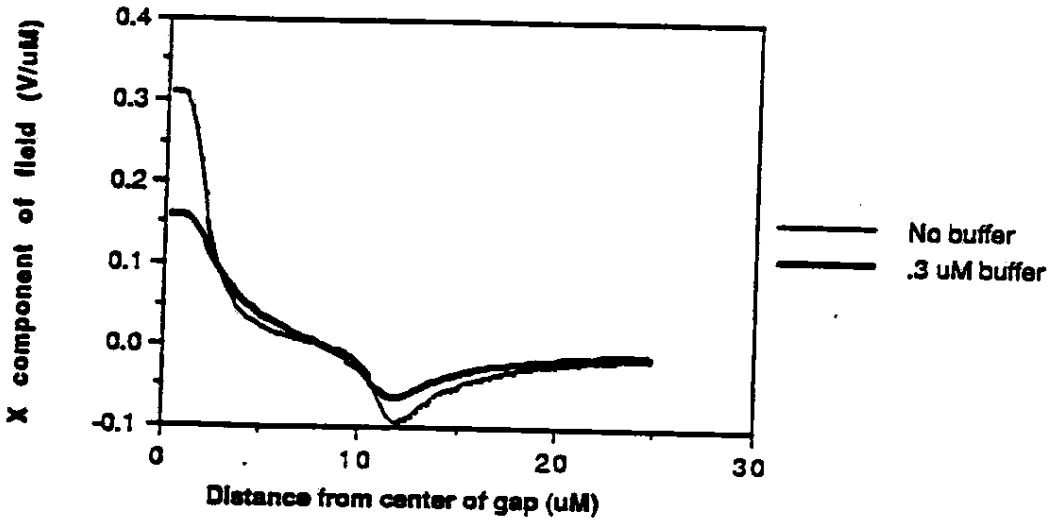

Figure 9: Effect of buffer layer on x component of electric field

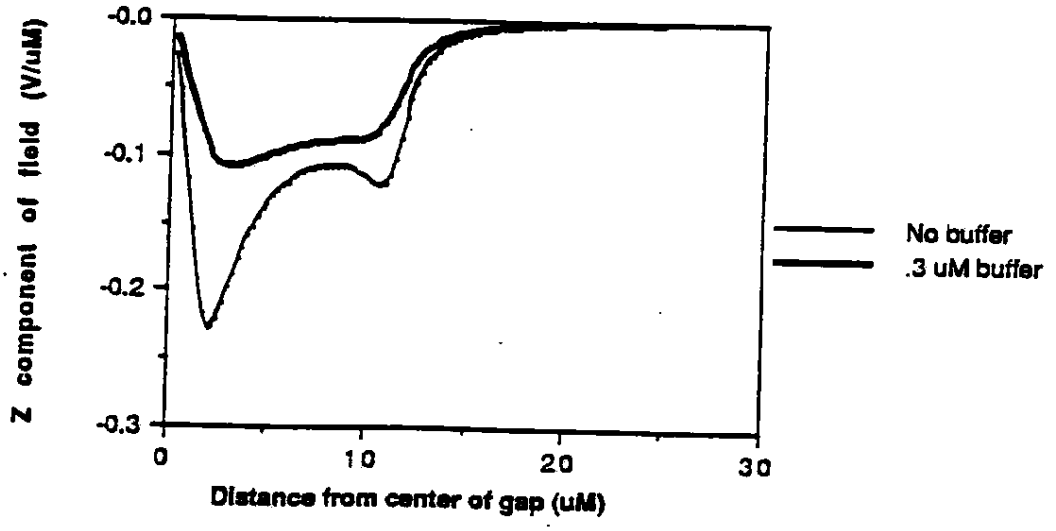

Figure 10: Effect of buffer layer on z component of electric field

Figures 9 and 10, it is obvious that even a very small ~0.3 micron buffer layer can produce 3 dB of attenuation of the field components.

6 Approximation for Symmetric Electrodes

The numerical technique described in the preceding section provides an excellent tool for accurately analyzing any type of coplanar electrode structure. Unfortunataly, the computations required to achieve significant results are extremely lengthy. In the example of the previous section, 350 basis functions were required on the symmetric electrode structure to converge to the correct charge density. This resulted in a 350 by 350 $[L]$ matrix. Filling up this dense matrix and inverting it takes approximately one hour on a HP300 workstation. While this is fast enough to analyze single devices, it is prohibitively slow for use in a CAD system where on-line changes in a circuit can be analyzed and parameters quickly recalulated.

Once the charge distribution on the electrodes is calculated, the following steps of calculating the static capacitance per unit length, and electric fields in the substrate can be done very quickly using equations 41, 46, and 47. The problem then was to find an approximation for the charge distribution

on the electrodes as a function of buffer layer thickness.

After observing the effect of changing the buffer layer thickness on the charge distribution, it was obvious that increasing the buffer layer thickness had the effect of decreasing the total charge density while at the same time, causing a more rapid change in charge density near the edges of the strips. The point at which the charge density starts to rapidly increase also moves closer to the edge of the strip as the buffer layer thickness is increased. This is displayed in figures11 and 12. We then observed that this is the same effect that changing the substrate thickness of a microstrip has on the microstrip charge density as observed by Kobayashi [10]. The dependance of microstrip charge density vs Width to height ratio is shown in figures 13 and 14.

Kobayashi derives a closed-form expression for the charge distribution on a microstrip by starting with the charge distribution on a strip in free space at a fixed potential. Since this gives the general shape of the charge distribution, he only needs to perturb it slightly to account for the effect of the substrate thickness and ground plane. Our approach is very similar. The total charge distribution on the coplanar electrode structure can be approximated in closed form by Kuester's expression for capacitance which is

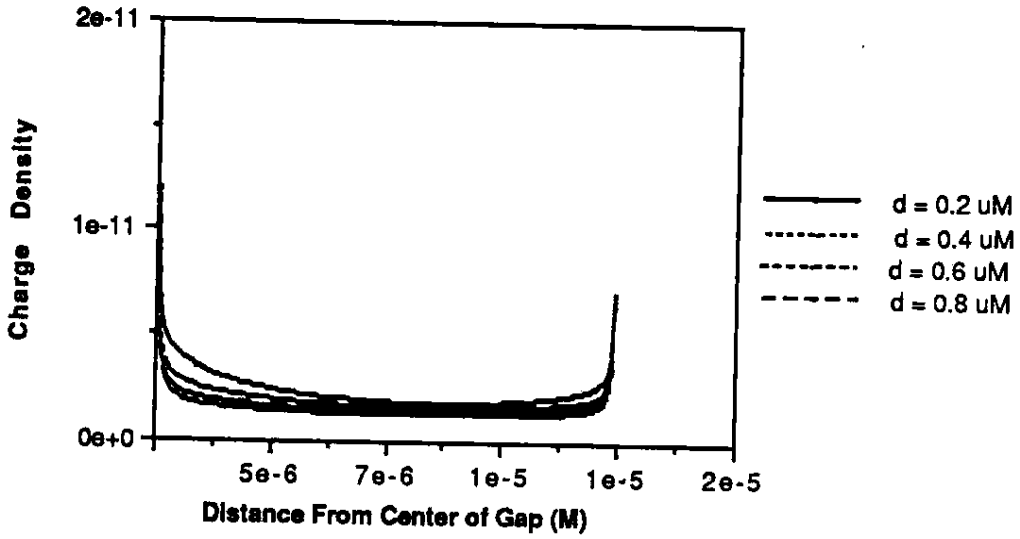

Figure 11: Effect of buffer layer thickness on charge density

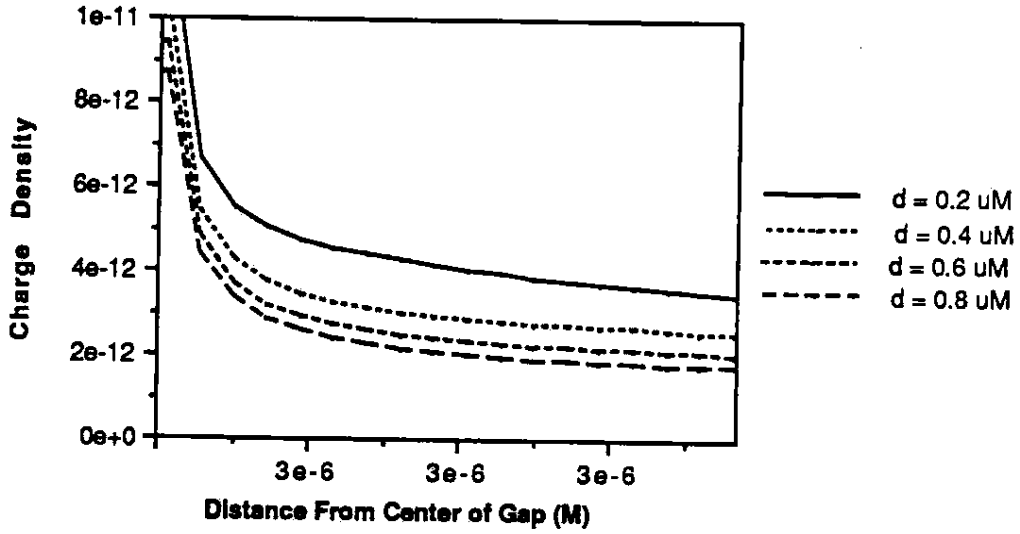

Figure 12: Effect of buffer layer thickness on charge density near edge of electrode

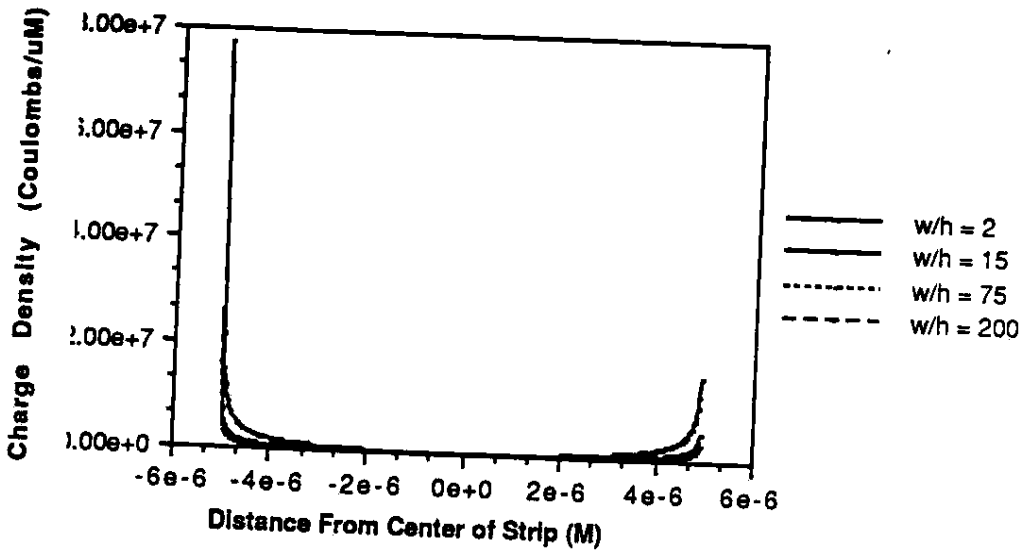

Figure 13: Effect of substrate thickness on microstrip charge density

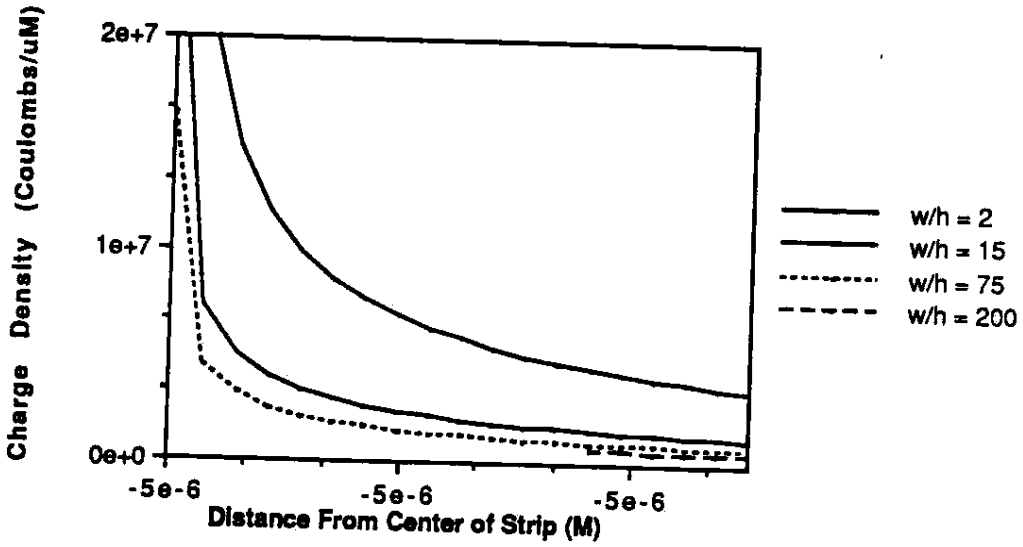

Figure 14: Effect of buffer layer thickness on charge density near edge of strip

given in equation 42. It remains then to find an approximation for the shape of the charge distribution as a function of buffer layer thickness. We start with the charge distribution on a symmetric coplanar electrode structure in a two layer system. This expression is derived exactly, in closed form in Kuester's report [5]. Since we are only concerned with the shape, we drop the constant from in front of the expression and are left with

$$\sigma_0(x) = \frac{1}{\sqrt{(b^2 - x^2)(x^2 - a^2)}} \tag{50}$$

where $a = g/2$ and $b = w + g/2$

The next step is to use Kobayashi's formula describing the change in charge distribution on a microstrip as W/H changes, but substituting the expression for the charge distribution on coplanar strips in place of that for microstrip in free space. The equation for the shape of the charge distribution then becomes.

$$\sigma(x) = 1 + 10(1 - \frac{2x_c}{w})\frac{\sigma_0(x) - 1}{\sigma 0(x_c) - 1} \tag{51}$$

Where x_c is the location where the charge distribution starts to rapidly increase near the edge of the electrodes. The effect of the electrode width to gap ratio is accounted for in equation 50. The only thing left to do is to

find X_c as a function of the buffer layer thickness. This was accomplished by finding the charge distribution numerically, then using a least squares error analysis program, computing the X_c which gives the minimum error for the given geometry. This procedure was done for 20 different buffer layer thicknesses, then a curve fitting program was used to get X_c as a function of buffer layer thickness, and electrode width.

The formula obtained is the following

$$\frac{X_c}{w} = 0.45564 + 0.10364\frac{w}{h} \quad \frac{w}{h} < 25 \tag{52}$$

$$-8.9386e-3(\frac{w}{h})^2 + 3.4427e-4(\frac{w}{h})^3 - 4.9056e-6(\frac{w}{h})^4 \tag{53}$$

$$\frac{X_c}{w} = 0.89679 + 2.3184e-3\frac{w}{h} \quad \frac{w}{h} \geq 25 \tag{54}$$

$$-6.4321e-3(\frac{w}{h})^2 + 5.9288e-7(\frac{w}{h})^3 - 2.083e-9(\frac{w}{h})^4 \tag{55}$$

This function is plotted in figure 15.

We now have everything we need to compute the charge density on any symmetric coplanar electrode structure using equation51 multiplied by a constant to set the total charge distribution equal to that found in equation 42. Figure16 shows the charge distribution on symmetric 10 micron electrodes,

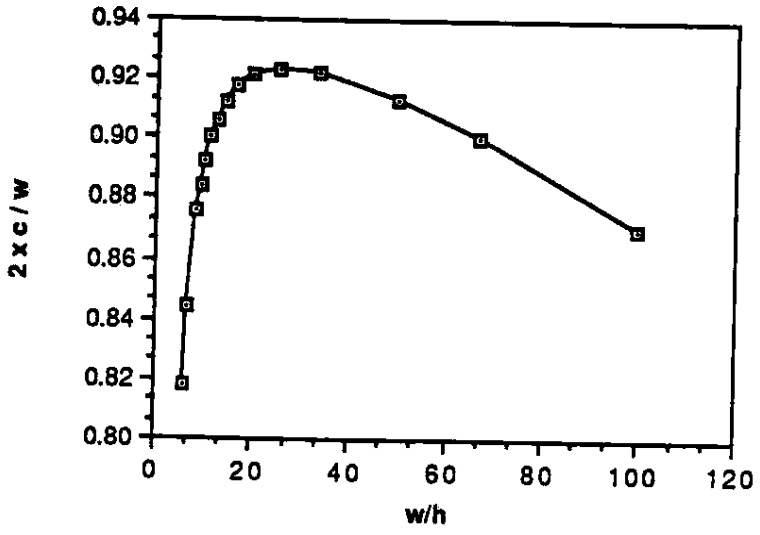

Figure 15: Width to buffer layer thickness ratio effect on $\frac{X_c}{w}$

with a 3 micron gap and a 0.3 micron buffer layer, computed numerically using the technique described earlier and the approximate technique. Although the approximation is slightly in error in some places, it will be integrated to find the electric fields, which reduces the error considerably.

Once the charge distribution has been approximated, we use the technique described in the previous section to compute the fields from this approximate charge distribution. Figures 17 and 18 show the X and Z components of Electric field in a ten micron symmetric structure with a 3 micron gap and 0.3 micron buffer layer using the numerical technique from the previous section

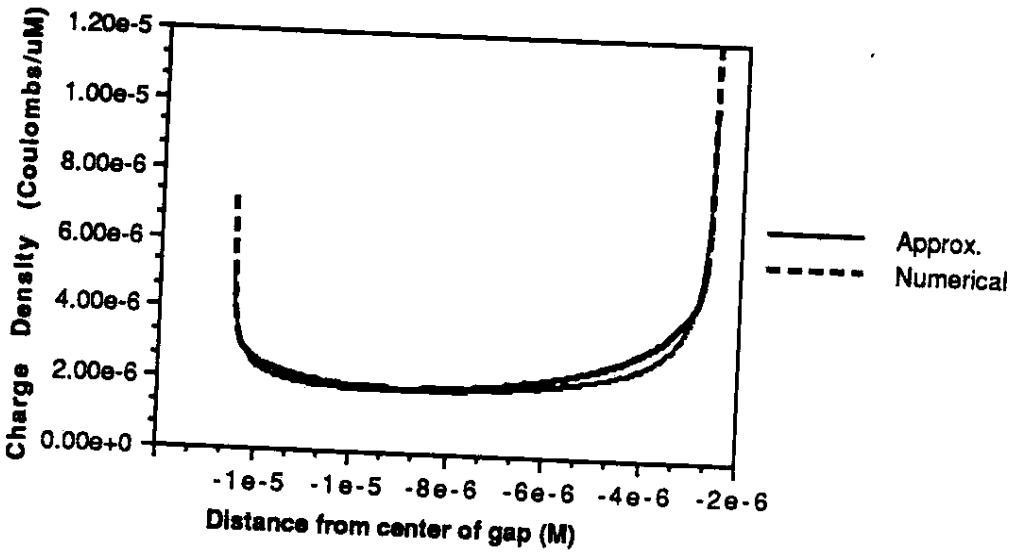

Figure 16: Comparison of charge distribution computed numerically and with approximation

and the approximate technique described above. The errors in the approximation are very small, much lower than the errors in the charge distribution due to the integration. Figures 18 - 22 Show numerical vs approximation of fields for two other geometries, first the gap is changed and then the buffer layer thickness is changed. Typically buffer layers are made as thin as possible, and gaps as narrow as possible to produce the strongest electric fields. This approximation produces very good results for all reasonable buffer layer thicknesses and gap widths. buffer layer thicknesses and gap

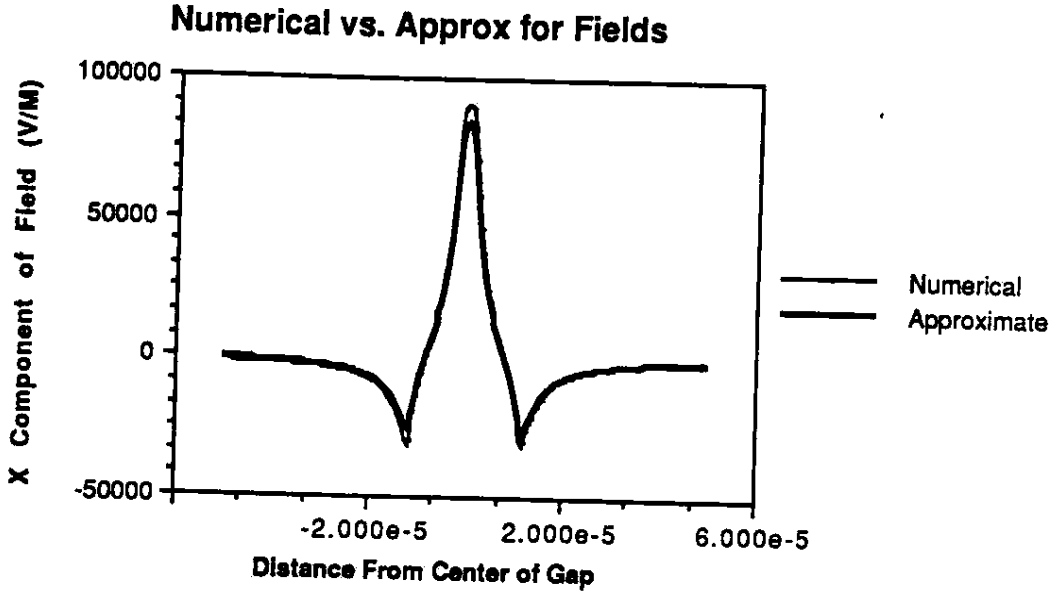

Figure 17: X component of field, numerical vs approximation, W = 10, G = 3, D = 0.3

7 Conclusions

Placing a dielectric buffer layer between the electrodes and substrate of an electroopic device changes many of the properties of the electrodes. The electric fields in the substrate are greatly reduced by adding even a very thin buffer layer. This means that the depth of modulation obtained for a given voltage is also greatly reduced. Due to this effect it is advantageous to use ITO electrodes which require no buffer layer when the amount of microwave power available is a concern. Adding a dielectric buffer layer also

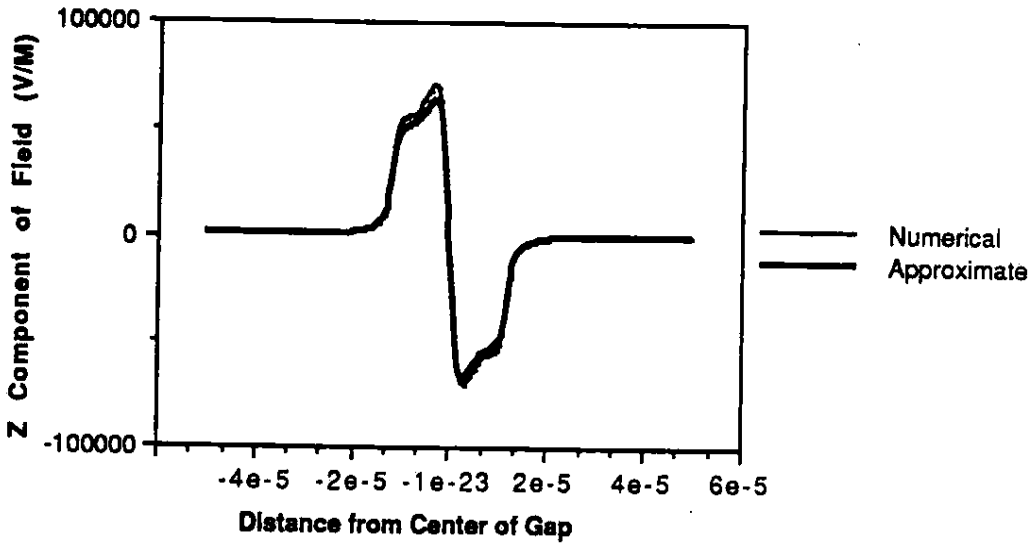

Figure 18: Z component of field, numerical vs approximation, W = 10, G = 3, D = 0.3

has the effect of lowering the static capacitance per unit length of the electrode structure. If the capacitance is lowered, the microwave phase velocity is increased. This could be a solution to the problem of the mismatch in phase velocity between the microwave and optical signals which limits the highest operating frequency of these devices.

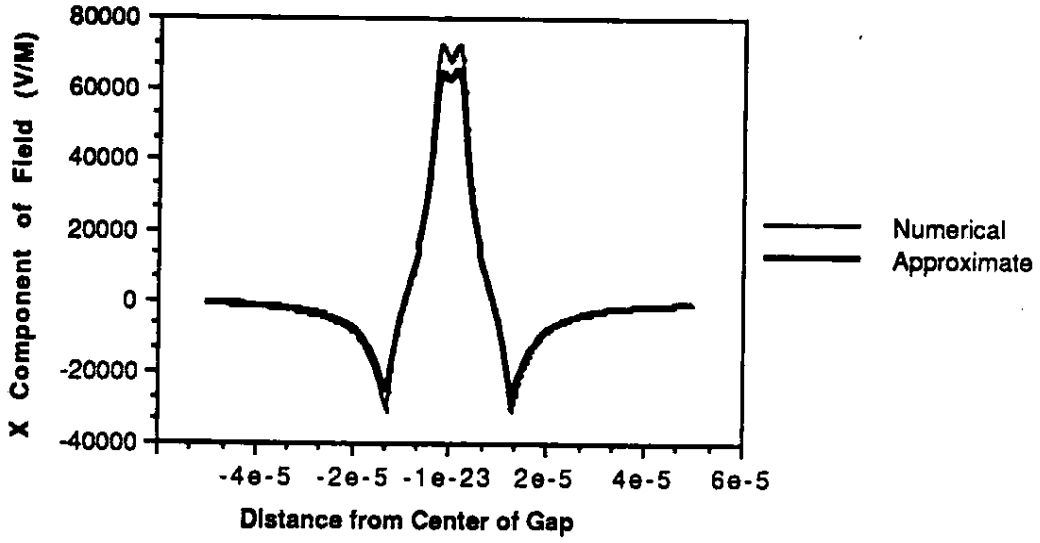

Figure 19: X component of field, numerical vs approximation, W = 10, G = 5, D = 0.3

8 Future work

Currently, these numerical programs require considerable computer time. The algorithms could be considerably improved by using more accurate basis functions when computing the charge distribution. The more accurate basis functions could also model the charge distribution near the electrode edges more accurately, giving better results. The procedure outlined above can accurately model any continuous coplanar configuration of electrodes, however a model is needed for discontinuities in coplanar electrode structures.

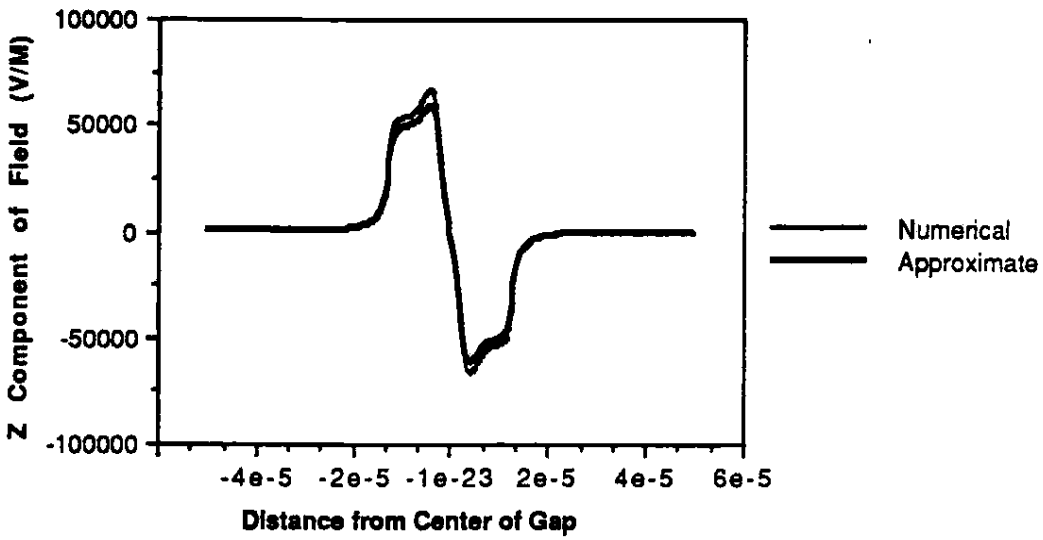

Figure 20: Z component of field, numerical vs approximation, W = 10, G = 5, D = 0.3

The quasistatic approximation used in all the calculations in this paper will eventually break down if the frequency is increased enough. With the increasing demand for faster electrooptic devices, a full dispersion analysis of such electrode structures will soon be neccessary.

References

[1] K. C. Gupta, R. Garg and I. J. Bahl, *Microstrip Lines and Slotlines.*, Dedham, MA: Artech House, 1979, chapter 7.

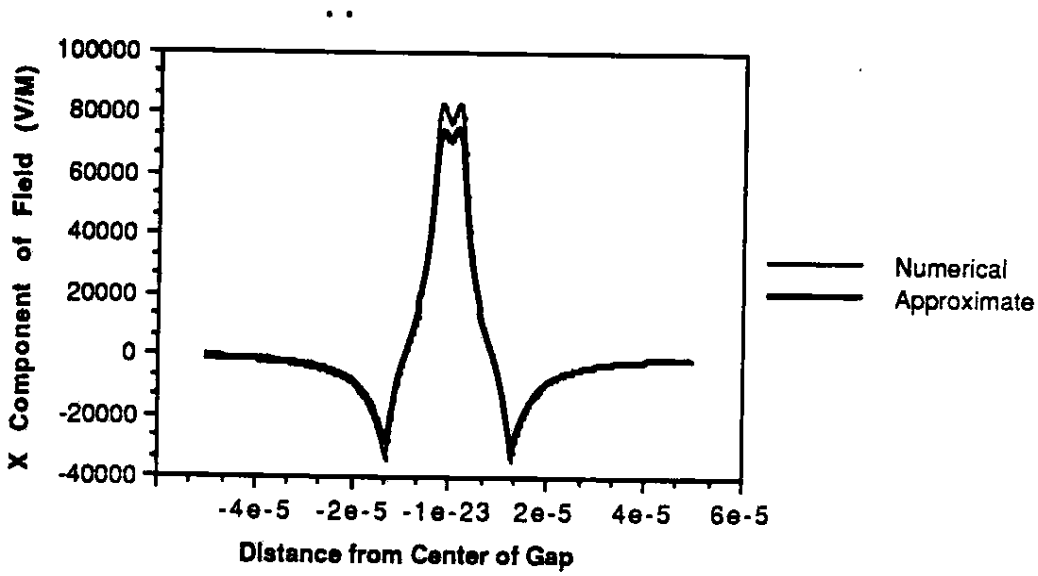

Figure 21: X component of field, numerical vs approximation, W = 10, G = 5, D = 0.2

[2] O. G. Ramer, "Integrated optic electrooptic modulator electrode analysis," *IEEE J. Quantum Electron.*, vol. QE-18, pp. 386-392, 1982.

[3] J. B. Knorr and K. Kuchler, "Analysis of Coupled Slots and Coplanar Strips on Dielectric Substrate," *IEEE Trans. Micr. Theory Tech.*, vol. MTT-23, pp. 541-548, 1975.

[4] L. Thylen and P. Granestrand, "Integrated Optic Electrooptic Device Electrode Analysis: The Influence of Buffer Layers," *J. of Optical Communications.*, vol. 7, pp. 11-14, 1986.

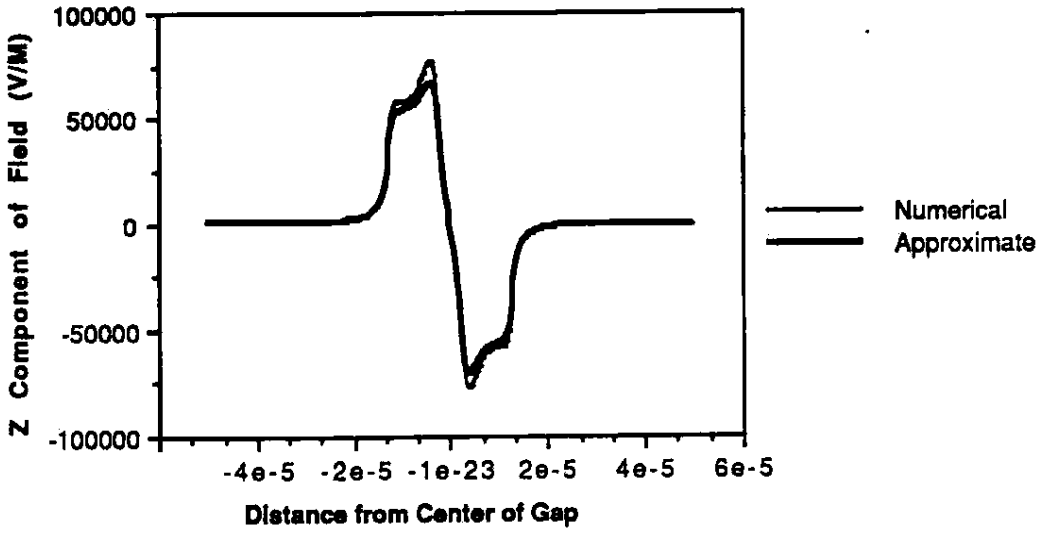

Figure 22: Z component of field, numerical vs approximation, W = 10, G = 5, D = 0.2

[5] E. F. Kuester, D. C. Chang and F. S. Quazi, "Line Parameters of Coplanar Strips Used as Electro-optic Modulator Electrodes," *University of Colorado Electromagnetics Laboratory Scientific Report No. 84*, 1986.

[6] D. Marcuse, "Electrostatic Field of Coplanar Lines Computed with the Point Matching Method," *IEEE J. of Quantum Elec.*, vol. 25, pp. 939-947, 1989.

[7] C. Sabatier and E. Caquot, "Influence of a Dielectric Buffer Layer on the Field Distribution in an Electrooptic Guided-Wave Device," *IEEE*

J. of Quantum Elec., vol. QE-22, pp. 32-36, 1986.

[8] I. S. Gradshteyn and I.M. Ryzhik, *Table of Integrals, Series and Products.*, p. 477, New York: Academic Press, 1965.

[9] E. Yamashita, K. Atsuki and T. Mori, "Application of MIC formulas to a Class of Integrated Optics Modulator Analyses: a Simple Transformation,"*IEEE Trans. Micro. Theory Tech.*, vol. 25, pp. 146-150 (1977).

[10] M. Kobayashi, "Longitudinal and Transverse Current Distributions on Microstriplines and thier Closed-Form Expression,"*IEEE Trans. Micro. Theory Tech.*, vol MTT-33, pp784-788 (1985).